ORIGINAL ARTICLE

Dynamic pathology for circulating free DNA in a dextran sodium sulfate colitis mouse model

**Yuhki Koike · Keiichi Uchida · Koji Tanaka · Shozo Ide · Kohei Otake ·
Yoshiki Okita · Mikihiro Inoue · Toshimitsu Araki · Akira Mizoguchi ·
Masato Kusunoki**

Abstract

Purpose In sepsis, circulating free DNA (cf-DNA) is
increased, and is a marker of severity and prognosis of
septic patients. This study aimed to evaluate cf-DNA in a
dextran sodium sulfate-induced colitis mouse model, and
its clinical implications.

Methods Dynamic pathology of the cecum wall in the
DSS-induced colitis mouse model was analyzed using
multiphoton microscopy (MPM). Plasma cf-DNA concen-
trations in colitis mouse were quantified using PicoGreen
dsDNA Assay Kit. Plasma cf-DNA was also measured in
123 human ulcerative colitis (UC) patients [mean age:
35.9 years (3–75 years) with 20 pediatric patients] to
assess its relationships with clinical severity and Matt's
grade.

Results Real-time images of cf-DNA were detected in the
colitis model. The amount of labeled cf-DNA in the cir-
culation of the colitis mice group was significantly higher
compared with that in the control group ($P < 0.05$). In
human UC blood samples, plasma cf-DNA concentrations
in UC patients were significantly positively correlated with

the clinical severity of UC and Matt's grade ($P < 0.05$,
$P < 0.05$, respectively).

Conclusions Using MPM, we observed and analyzed
real-time images of cf-DNA in a colitis mouse model.
Plasma cf-DNA is a potential non-invasive blood marker
for reflecting clinical severity and mucosal damage in UC
patients.

Keywords Green fluorescent protein · Multiphoton
fluorescence microscopy · Circulating free DNA,
neutrophils · Sepsis · Time-lapse imaging

Y. Koike (✉) · K. Uchida · K. Tanaka · S. Ide · K. Otake ·
Y. Okita · M. Inoue · T. Araki · M. Kusunoki
Department of Gastrointestinal and Pediatric Surgery, Mie
University Graduate School of Medicine, 2-174 Edobashi, Tsu,
Mie 514-8507, Japan
e-mail: koikyon@clin.medic.mie-u.ac.jp

A. Mizoguchi
Department of Neural Regeneration and Cell Communication,
Mie University Graduate School of Medicine, 2-174 Edobashi,
Tsu, Mie 514-8507, Japan

Introduction

Under conditions of sepsis, circulating free DNA (cf-DNA)
is increased, and is reported to be a marker of severity and
prognosis in septic patients [1, 2]. Neutrophils, eosinophils,
and macrophages release cf-DNA as a result of apoptosis
or other forms of cellular damage [3]. Levels of plasma cf-
DNA are increased in inflammation and cell death. Previ-
ous studies have shown that increased levels of cf-DNA are
extremely sensitive and specific for poor outcomes, other
than septic conditions. Circulating free DNA has prog-
nostic relevance in trauma [4], stroke [5], cancer [6], dia-
betes mellitus, and organ transplantation [7].

Recently, under conditions of sepsis, some researchers
have reported that cf-DNA is also released from a specific
phenomenon called neutrophil extracellular traps (NETs)
[8, 9]. In NETs, neutrophils release their granular proteins
and chromatin, and together form extracellular fibers that
bind Gram-positive and Gram-negative bacteria. The pro-
cess of NET formation is pathologically and morphologi-
cally distinct from other classical cell death processes,
including apoptosis and necrosis. Therefore, this process is

called "NETosis", which is characterized by fibrous mesh-like or web-like structures, and these are composed of DNA, histones, and granule proteins, such as neutrophil elastase or myeloperoxidase [10]. NET formation has also been observed in chronic inflammatory conditions, such chronic obstructive pulmonary disease [11] and ulcerative colitis (UC) [12]. NET formation has only been observed in vitro in UC.

We have reported and standardized the methods of in vivo real-time imaging for intra-abdominal organs and microcirculation of the intestine using multiphoton microscopy (MPM) with an organ-stabilizing system [13–18]. Use of MPM has revolutionized in vivo real-time imaging because of its benefits of higher resolution, increased tissue penetration, and reduced photo-damage compared with confocal microscopy [19, 20]. This system allows high-magnification, high-resolution images of exteriorized living tissue to be captured from the surface to several micrometers in depth [13–18, 21]. We have previously visualized in vivo real-time colorectal liver metastatic formation [15], three-dimensional steroid efficacy for DSS-induced colitis [16], thrombus formation in laser-induced endothelium injury [17], bacterial translocation in dextran sodium sulfate (DSS)-induced colitis [18], and chemotherapy responses to the tumor microenvironment of colorectal liver metastases [13, 14, 21].

In this study, we visualized and characterized cf-DNA and NETs real-time in vivo in a DSS-induced colitis model of green fluorescent protein (GFP) transgenic mice by using MPM. We also investigated blood cf-DNA concentrations in the DSS-induced colitis mouse and human UC patients, and examined its clinical implications.

Materials and methods

Transgenic mice

Wild-type C57/BL6 mice and enhanced GFP (EGFP)-transgenic C57/BL6-Tg (CAG-EGFP) mice [23] were purchased from Japan SLC (Shizuoka, Japan). The 10- to 15-week-old male mice (body weight: 20–25 g) were bred, housed in groups of six mice per cage, and fed with a pelleted basal diet (CE-7; CLEA Japan, Tokyo, Japan) and had free access to drinking water. Mice were kept in the animal house facilities at the Mie University School of Medicine under standard conditions of humidity (50 ± 10 %), temperature (23 ± 2 °C), and light (12/12-h light/dark cycle), according to the Institutional Animal Care Guidelines. The experimental protocols were reviewed and approved by the Animal Care and Use Committee at the Mie University Graduate School of Medicine.

DSS-induced colitis model

Mice allocated to the DSS treatment group ($n = 10$) had 2 % (w/v) DSS (MP Biomedicals, Solon, OH, USA; MW 36,000–50,000) added to their drinking water for 7 days (after 7 days, distilled water was provided). Control mice ($n = 10$) drank distilled water for 7 days.

Setup of MPM

Experiments were performed using an upright microscope (BX61WI; Olympus, Tokyo, Japan) and a FV1000-2P laser-scanning microscope system (FLUOVIEW FV1000MPE; Olympus, Tokyo, Japan) as described previously [17, 18]. The excitation source was a Mai Tai Ti:sapphire laser (Spectra Physics, Mountain View, CA, USA), which was tuned and mode-locked at 910 nm. The 60× LUMPlanFI/IR (water dipping; numerical aperture, 0.9; working distance, 2 mm) or 20× UPlanSApo (numerical aperture 0.75) microscope objective lens was used. Data were analyzed using the FV10-ASW system (Olympus). MPM images were acquired with 512 × 512 pixels of spatial resolution from a 211-μm field of view dimension using a pixel dwelling time of 4 μs.

Surgical procedures for in vivo real-time imaging

As previously described [19–22], GFP mice were anesthetized with isofluorane 4 L/min (4 %; Forane, Abbott, Japan). Body temperature was maintained at 37 °C using a heating pad. For imaging post capillary venules (NETs phenomenon mainly occurred in this area), the cecum was identified and exteriorized through laparotomy. The exteriorized cecum was optimally inflated by introducing air using a syringe with a small-bore needle. The inflated cecum was placed on an organ-stabilizing system (Japanese Patent No. 5268282) to reduce the effect of heartbeat and respiratory movements.

Antibodies and reagents

Goat anti-mouse neutrophil elastase (NE) antibodies were purchased from Santa Cruz Biotechnology (Santa Cruz, CA, USA). SYTOX Orange nucleic acid stains and Zenon Alexa Fluor immunoglobulin G (IgG) labeling kits were purchased from Invitrogen (Carlsbad, CA, USA) [9].

Imaging methods

The surface of the cecum was screened at low magnification to identify the optimal observation area [14–17, 21]. The areas of interest were scanned at higher magnification (water-immersion objective 60× with or without 2× zoom) to obtain high-resolution and clear MPM images. The

imaging depth was determined arbitrarily, by adjusting the laser power. In our experimental setting, the imaging depth ranged from 100 to 400 μm. Optimal high resolution images were obtained from the tissue surface up to 100–200 μm in depth. For optimal simultaneous imaging of EGFP and Alexa Fluor 594, detection sensitivity was adjusted for EGFP (to 485–510 nm) or Alexa Fluor 594 (to 585–635 nm).

Visualization of cf-DNA, NETs, and NE in vivo by MPM

To administer regents precisely and reliably, a catheter (M-FAC/FVC, Neuroscience, Tokyo, Japan) was placed in the femoral vein of the anaesthetized mice under surgical microscopy. After laparotomy, the cecum was exteriorized and fixed using the organ-stabilizing system. After identifying optimal areas, SYTOX Orange, or Alexa Fluor 594-labeled anti-NE antibodies were administered intravenously via a catheter. NETs, NE, and cf-DNA were detected and visualized in living mice. Color-coded green (EGFP) and red (SYTOX Orange and Alexa Fluor 594) images were recorded at the same time. Subsequently, they were merged to produce single dual-color images.

Quantification of cf-DNA and NE by intravital MPM imaging

Intravascular cf-DNA was identified by a cell impermeable DNA dye, SYTOX orange, and NE was identified by Alexa Fluor 594-labeled anti-NE antibody. The numbers of labeled cf-DNA and NE were counted in 10 randomly selected fields (600×; 211 × 211 μm square) with intravital MPM imaging for 30 s. The average number per field (211 × 211 μm square) was expressed as the number of labeled cf-DNA and NE per field of view.

Quantification of NETs by intravital MPM imaging

Intravascular NETs were identified by SYTOX Orange. The number of NETs present in intravascular spaces was counted in 10 randomly selected fields (600×; 211 × 211 μm square) with intravital MPM imaging. The sum of this count (a total number of 10 fields) was expressed as the number of NETs per field of view.

Quantification of plasma cf-DNA and NE concentrations

Heparinized blood was obtained from control (DSS-untreated), 2 % DSS-treated mice [5–10 mice at each time point (days 0, 7, and 14 from the start of drinking distilled water or 2 % DSS)], and preoperative (subtotal colectomy or total colectomy) human UC patients (n = 123). Heparinized blood samples were separated by centrifugation and stored at −80 °C until analysis. Plasma DNA was quantified using a Quant-iTTM PicoGreen dsDNA Assay Kit according to the manufacturer's instructions. In brief, plasma was diluted tenfold with Tris–EDTA buffer and mixed with an equal volume of PicoGreen reagent. The PicoGreen dye that was bound to double-stranded DNA was measured using a fluorescence microplate reader (2030 ARVO X; Perkin Elmer, Waltham, MA, USA). The DNA concentration was calculated using a standard curve generated from a series of Lambda DNA standard (100 μg/ml) provided by the manufacturer. NE was measured using an ELISA kit (Immundiagnostik AG, Bensheim, Germany) according to the manufacturer's instructions.

Analysis of the clinical implications of cf-DNA in human UC patients

Three hundred twenty-one consecutive patients undergoing subtotal colectomy or total colectomy for UC from 2000 to 2012 at Mie University Hospital were enrolled in this study. The study was conducted in accordance with the guidelines of the 1975 Declaration of Helsinki. Diagnosis and assessment of bowel involvement were based on clinical, radiographic, endoscopic, and pathological data. Patients with preoperative clinical symptoms of sepsis were excluded. The extent and severity of UC were classified by Montreal classification [22]. Preoperative blood samples were obtained in 123 patients. After measurement of the number of circulating lymphocytes and neutrophils, plasma was separated by centrifugation and stored at −80 °C until assay. Plasma concentrations of NE were measured using an ELISA kit (Immundiagnostik AG) according to the manufacturer's instructions.

Characteristics of UC patients

To validate the clinical implications of cf-DNA, we measured blood cf-DNA concentrations in preoperative UC patients (n = 123). The baseline characteristics of the 123 UC patients are shown in Table 1. Of the 123 patients, 20 were under 15 years old. With regard to Montreal classification of these patients, mild UC (S1) was found in 52, moderate UC (S2) in 39, and severe UC (S3) in 32 patients. With regard to Matt's classification (endoscopic severity grade), 21 patients had grade 1, 51 had grade 2, 25 had grade 3, and 15 had grade 4.

Statistical analysis

Statistical analyses were performed using JMP version 5 (SAS Institute Inc. Cary, NC, USA). The data are shown as

Table 1 Characteristics of UC patients

Mean age ± SD (range)	35.9 ± 1.52 (3–75)
Sex (male/female)	72/51
Montreal classification of UC severity	
Mild	52
Moderate	39
Severe	32
Matt's classification	
1	21
2	51
3	25
4	15

the mean + standard error (SE) and were analyzed by the Mann–Whitney U test. A P value of less than 0.05 was considered statistically significant.

Results

Visualization of cf-DNA and NETs in DSS-induced colitis mice and control mice

Intravascular cf-DNA and NETs were identified with SY-TOX orange by our MPM system (Fig. 1a, b, see also supplementary movie file A and B). To compare the counts
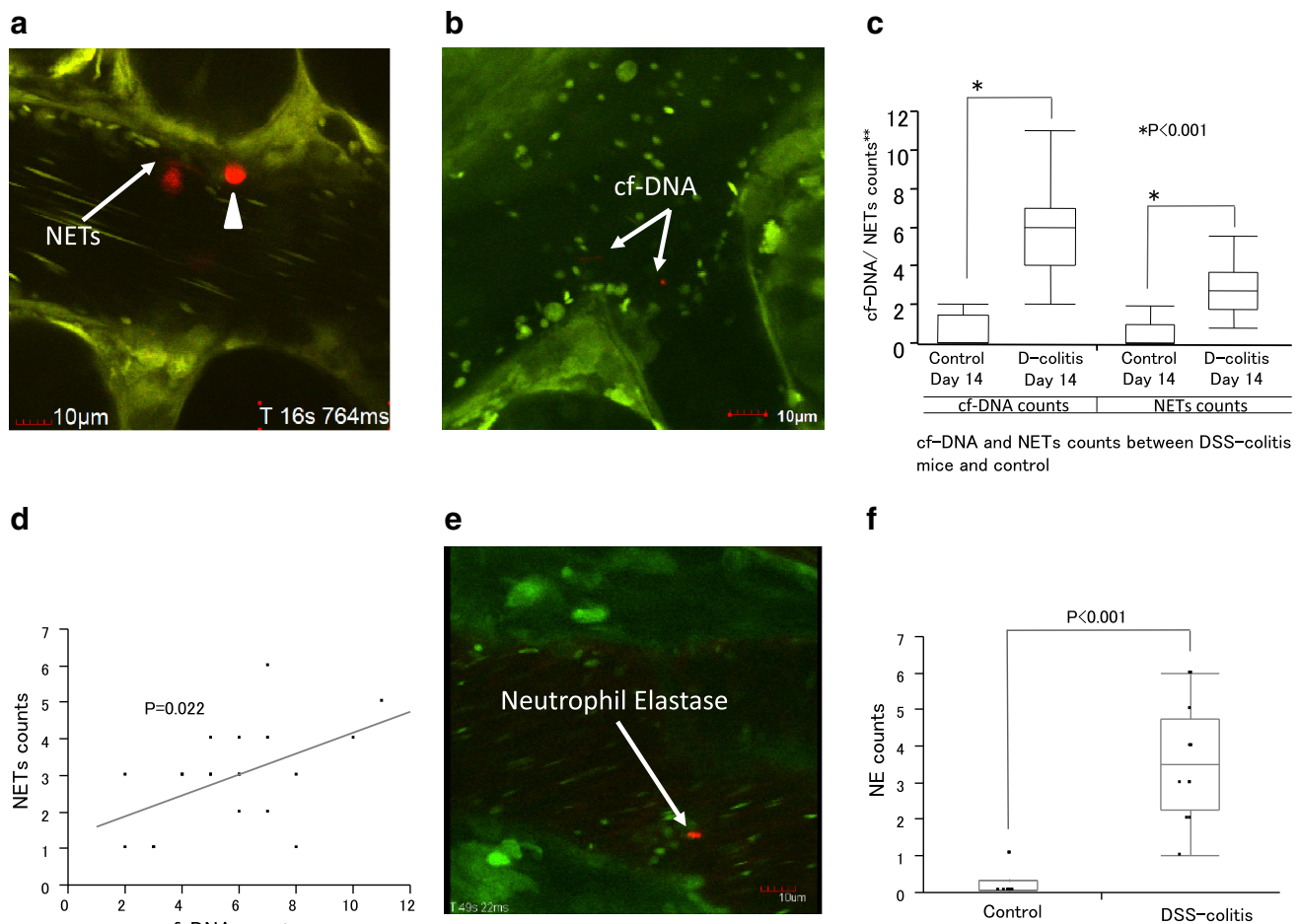

Fig. 1 **a**, **b** Intravascular NETs (**a**) and cf-DNA (**b**) (*red* indicated by the *white arrow*, the *white arrowhead* indicated the precondition of NETs released from neutrophil) were identified with SYTOX *orange* by our MPM system. **c** The presence rate per 30 s of labeled cf-DNA and NETs was significantly higher in DSS-induced colitis mice (day 14) compared with that of control mice ($P < 0.05$). **d** The number of labeled cf-DNA in the circulation was significantly correlated with the number of labeled NETs. **e** Intravascular circulating free NE (*red* indicated by the *white arrow*) was identified by Alexa Fluor 594-labeled anti-NE antibody by our MPM system. **f** The number of labeled NE in the circulation of DSS-induced colitis mice was

significantly higher compared with that in control mice. D-colitis, DSS-induced colitis mice. *Double asterisk* indicates the number of labeled cf-DNA was counted in 10 randomly selected fields (×600; 211 × 211 μm square) with intravital MPM imaging for 30 s. The average number per field (211 × 211 μm square) was expressed as the number of labeled cf-DNA per field of view (FOV). The number of NETs present in intravascular spaces was counted in 10 randomly selected fields (×600; 211 × 211 μm square) with intravital MPM imaging. The sum of them (a total number of 10 fields) was expressed as the number of NETs per field of view (FOV)

Fig. 2 Time course of plasma cf-DNA concentrations from day 0 to day 14 with or without DSS administration. Plasma cf-DNA concentrations were similar between DSS-induced colitis mice and controls at day 0. However, plasma cf-DNA concentrations in DSS-induced colitis mice were higher at days 7 and 14 compared with those in control mice. In their cage, DSS-induced colitis mice had the symptoms of anal bleeding and hematochezia on days 7 and 14. *D-colitis* DSS-induced colitis mice
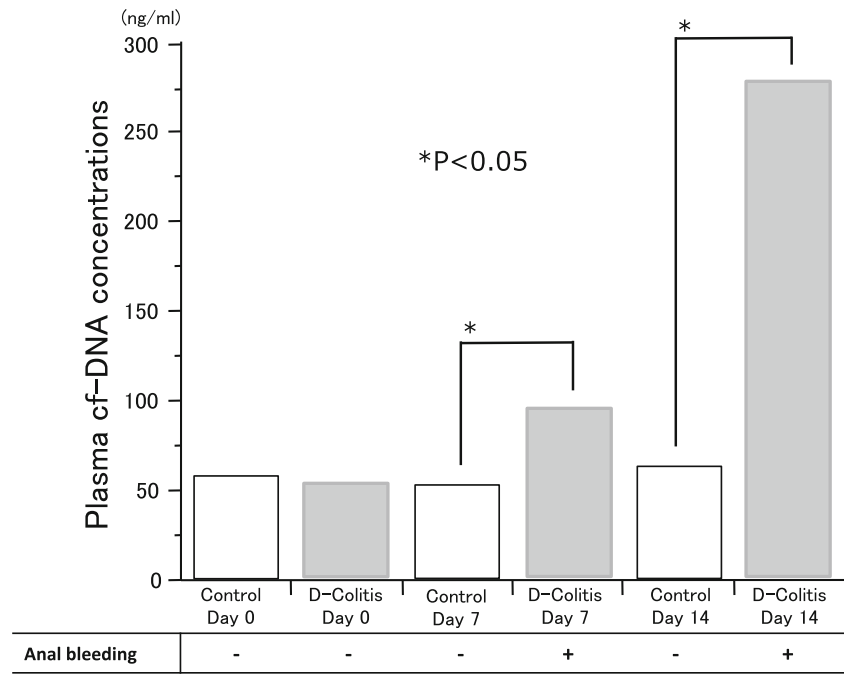
of cf-DNA and NETs between the DSS-induced colitis model and control mice by intravital MPM imaging, we quantified their amount at day 14 from the start of drinking distilled water or 2 % DSS (this point showed the highest rate of occurrence of cf-DNA and NETs, with severe anal bleeding, compared with those of day 7). Labeled cf-DNA was significantly higher in DSS-induced colitis mice (day 14) compared with that in control mice (Fig. 1c, $P < 0.001$). This finding was also observed in labeled NETs between DSS-induced colitis mice and control mice (Fig. 1c, $P < 0.001$). Moreover, in the in vivo colitis model, the number of labeled cf-DNA in the circulation was significantly correlated with the number of labeled NETs (Fig. 1d, $P = 0.022$).

Visualization of NE in DSS-induced colitis mice and control mice

Intravascular circulating free NE was identified by Alexa Fluor 594-labeled anti-NE antibody by our MPM system (Fig. 1e). The number of labeled NE in the circulation of DSS-induced colitis mice was significantly higher compared with that in control mice (Fig. 1f, $P < 0.001$).

Plasma cf-DNA concentrations in the DSS-induced colitis model

The time course of blood cf-DNA concentrations in the DSS-induced colitis model and controls is shown in Fig. 2. Blood cf-DNA concentrations were similar between
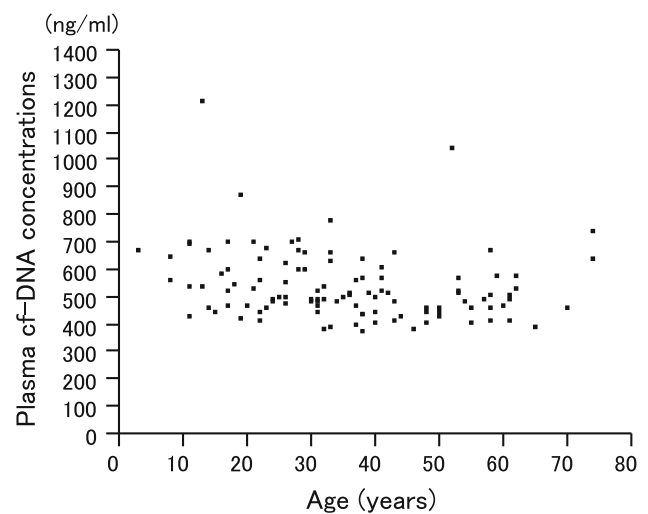

Fig. 3 Distribution of plasma cf-DNA concentrations. There was no significant relationship in the distribution of plasma cf-DNA concentrations between children (<15 years old) and adults

DSS-induced colitis mice and control mice at day 0. However, cf-DNA concentrations were higher in DSS-induced colitis mice at days 7 and 14 compared with those of control mice ($P < 0.05$). In their cage, DSS-induced colitis mice had symptoms of anal bleeding and hematochezia on days 7 and 14.

Blood cf-DNA concentrations in UC patients

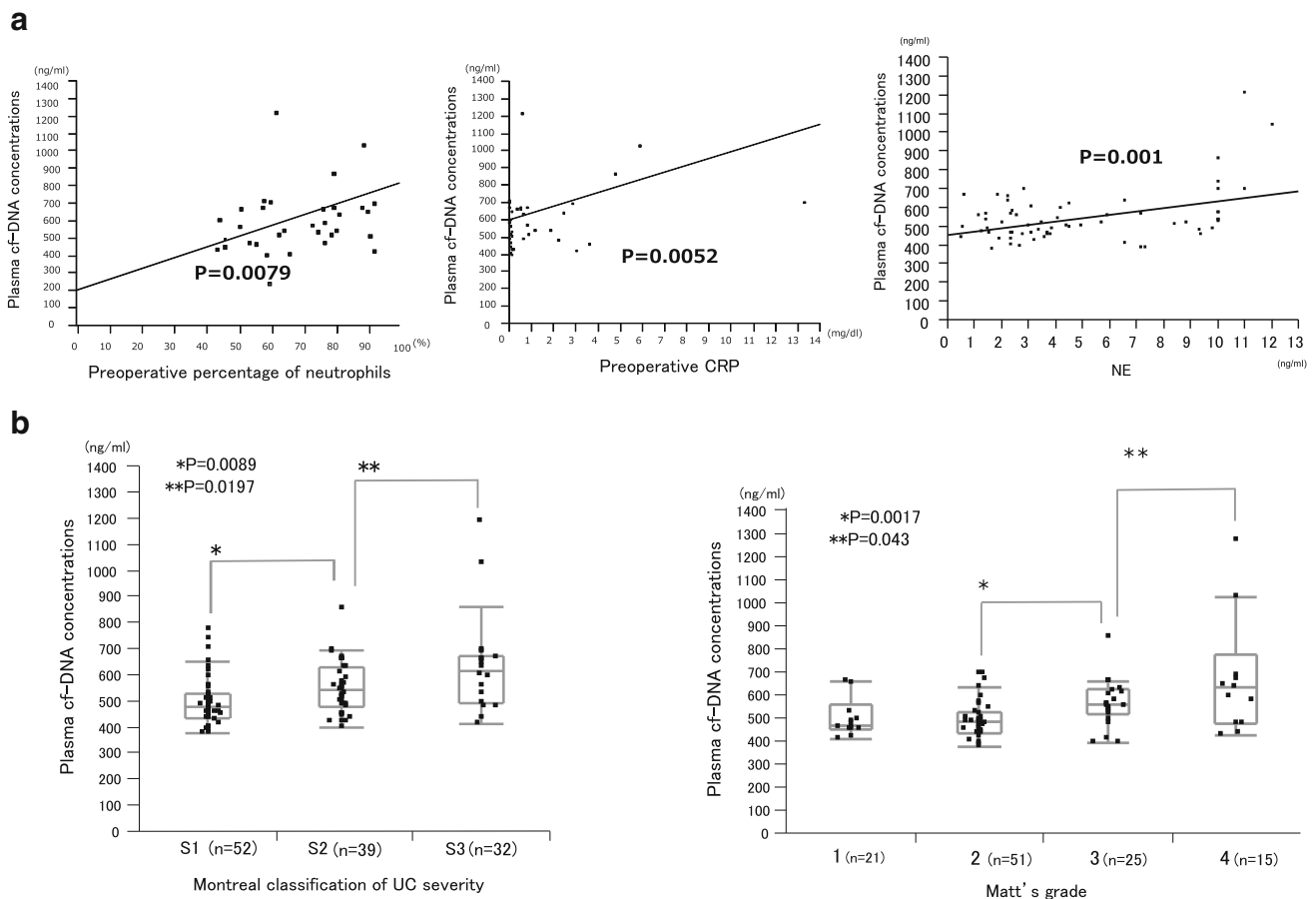Blood cf-DNA concentrations are plotted in Fig. 3. There was no significant relationship in the distribution of

Fig. 4 a Correlations between plasma cf-DNA concentrations and other inflammatory markers [percentage of neutrophils, C-reactive protein (*CRP*), and neutrophil elastase (*NE*)]. There were significant positive associations between cf-DNA and the percentage of neutrophils, CRP, and NE. **b** Correlations between plasma cf-DNA concentrations and the clinical severity of UC and Matt's grade. There were significant positive correlations between the amount of cf-DNA and these UC grades

cf-DNA concentrations between children (<15 years old) and adults.

Comparison of cf-DNA with the clinical severity of UC and other inflammatory factors

In human UC blood samples, plasma cf-DNA concentrations were significantly correlated with other inflammatory markers, such as the percentage of neutrophils ($P = 0.0079$), C-reactive protein ($P = 0.0052$), and NE ($P = 0.001$) (Fig. 4a). Moreover, plasma cf-DNA concentrations in UC patients were significantly positively correlated with the clinical severity of UC and Matt's grade ($P < 0.05$, respectively, Fig. 4b). In contrast, however other inflammatory markers (the percentage of neutrophils, C-reactive protein, and NE) had partially correlated with clinical severity of UC (positive correlation between S1 and S3), there was no significant correlations with Matt's grade (figure not shown).

Discussion

We achieved the direct visualization of cf-DNA and NET formation real time in vivo with high resolution imaging by using MPM in mice. We also showed that there was a positive correlation between the rate of occurrence of cf-DNA and NETs in DSS-induced colitis mice compared with those of controls. This is the first report of direct visualization of NET formation in an in vivo DSS-induced colitis model.

With regard to the association between UC and NETs, Alexander et al. [12] showed that NETs were released from neutrophils within crypt abscess lesions in UC patients, as shown by immunofluorescence in vitro. In this study, we showed in vivo NET formation in the DSS-induced colitis model for the first time. Moreover, in this model, we also showed a significant association between the rate of occurrence of NETs and cf-DNA.

Recently, NET research has pointed out another aspect of its adverse effect on the host, as well as the function of

extracellular trapping and killing pathogens. Previously, some researcher reported that NETs are associated with thrombogenesis [23, 24], atherosclerosis [25], autoimmune disease [26], and cancer metastasis [27]. Nuclear and granular proteins, which are contained in NETs, appear to induce NET-mediated host cell cytotoxicity [28]. These adverse effects of NETs on the host have also been reported with cf-DNA. There is increasing evidence that cf-DNA promotes inflammation, including systemic inflammation or inflammatory second hit [29–32], frailty [33], and thrombosis [24]. These characteristics of cf-DNA might have the aspect of alarmin [34]. The term "alarmin" is used for antimicrobial peptides that are chemotactic and able to respond to danger signals by alerting the immune system, as defined by Oppenheim et al. [34]. The effects of cf-DNA are mainly reported in acute inflammatory conditions, such as sepsis. Interestingly, in this study, we observed cf-DNA in UC patients who had acute and chronic inflammatory conditions. Moreover, increased cf-DNA concentrations were significantly positively associated with the Montreal classification of severity of UC and Matts' grade as endoscopic classification of UC. In UC patients, cf-DNA might be released from the inflammatory colitic mucosa or necrotic tissue, as suggested by Alexander et al. [12]. In our study, we showed that cf-DNA could also be released from NETs in UC patients. Therefore, this released cf-DNA might pass into the general circulation, and provoke a systemic inflammatory response or microcirculatory dysfunction. Based on these reasons, increased cf-DNA concentrations in UC patients might be a blood biomarker reflecting the severity of UC patients.

There are several limitations in our study, such as a limited imaging time and a limited observation area. However, this is the first report that has shown real-time MPM images in vivo, with high resolution of labeled cf-DNA and labeled NETs in a DSS-induced colitis mice model. We also showed a positive association between plasma cf-DNA concentrations and the severity of UC patients.

We observed that cf-DNA was elevated in DSS-induced colitis mice that had only localized inflammation of the colon. Therefore, other pediatric intestinal disorders, such as necrotizing enterocolitis, pediatric Crohn disease, and enteritis of Hirschsprung disease, might have elevated cf-DNA levels, reflecting some type of clinical severity. We plan to study these pediatric intestinal disorders in the future.

In conclusion, using MPM, we observed and analyzed real-time images of cf-DNA and NETs in a DSS-induced colitis mouse model. Plasma cf-DNA could be a potential non-invasive blood marker for reflecting the clinical severity and mucosal damage in UC patients.

References

1. Nakahira K, Kyung SY, Rogers AJ et al (2013) Circulating mitochondrial DNA in patients in the ICU as a marker of mortality: derivation and validation. PLoS Med 10(12):e1001577 (discussion e1001577)
2. Rhodes A, Cecconi M (2012) Cell-free DNA and outcome in sepsis. Crit Care 16(6):170
3. Huttunen R, Kuparinen T, Jylhava J et al (2011) Fatal outcome in bacteremia is characterized by high plasma cell free DNA concentration and apoptotic DNA fragmentation: a prospective cohort study. PLoS One 6(7):e21700
4. Lo YM, Rainer TH, Chan LY et al (2000) Plasma DNA as a prognostic marker in trauma patients. Clin Chem 46(3):319–323
5. Rainer TH, Wong KS, Lam W et al (2007) Comparison of plasma beta-globin DNA and S-100 protein concentrations in acute stroke. Clin Chim Acta 376(1–2):190–196
6. Elshimali YI, Khaddour H, Sarkissyan M et al (2013) The clinical utilization of circulating cell free DNA (CCFDNA) in blood of cancer patients. Int J Mol Sci 14(9):18925–18958
7. Butt AN, Swaminathan R (2008) Overview of circulating nucleic acids in plasma/serum. Ann N Y Acad Sci 1137:236–242
8. Brinkmann V, Reichard U, Goosmann C et al (2004) Neutrophil extracellular traps kill bacteria. Science 303(5663):1532–1535
9. Yipp BG, Petri B, Salina D et al (2012) Infection-induced NE-Tosis is a dynamic process involving neutrophil multitasking in vivo. Nat Med 18(9):1386–1393
10. Menegazzi R, Decleva E, Dri P (2012) Killing by neutrophil extracellular traps: fact or folklore? Blood 119(5):1214–1216
11. Obermayer A, Stoiber W, Krautgartner WD et al (2014) New aspects on the structure of neutrophil extracellular traps from chronic obstructive pulmonary disease and in vitro generation. PLoS One 9(5):e97784
12. Savchenko AS, Inoue A, Ohashi R et al (2011) Long pentraxin 3 (PTX3) expression and release by neutrophils in vitro and in ulcerative colitis. Pathol Int 61(5):290–297
13. Tanaka K, Toiyama Y, Okugawa Y et al (2014) In vivo optical imaging of cancer metastasis using multiphoton microscopy: a short review. Am J Trans Res 6(3):179–187
14. Tanaka K, Toiyama Y, Inoue Y et al (2013) Intravital imaging of gastrointestinal diseases in preclinical models using two-photon laser scanning microscopy. Surg Today 43(2):123–129
15. Tanaka K, Morimoto Y, Toiyama Y et al (2012) Intravital dual-colored visualization of colorectal liver metastasis in living mice using two photon laser scanning microscopy. Microsc Res Tech 75(3):307–315
16. Morimoto Y, Tanaka K, Toiyama Y et al (2011) Intravital three-dimensional dynamic pathology of experimental colitis in living mice using two-photon laser scanning microscopy. J Gastrointest Surg 15(10):1842–1850
17. Koike Y, Tanaka K, Okugawa Y et al (2011) In vivo real-time two-photon microscopic imaging of platelet aggregation induced by selective laser irradiation to the endothelium created in the

beta-actin-green fluorescent protein transgenic mice. J Thromb Thrombolysis 32(2):138–145

18. Toiyama Y, Mizoguchi A, Okugawa Y et al (2010) Intravital imaging of DSS-induced cecal mucosal damage in GFP-transgenic mice using two-photon microscopy. J Gastroenterol 45(5):544–553

19. Ustione A, Piston DW (2011) A simple introduction to multi-photon microscopy. J Microsc 243(3):221–226

20. Pittet MJ, Weissleder R (2011) Intravital imaging. Cell 147(5):983–991

21. Tanaka K, Morimoto Y, Toiyama Y et al (2012) In vivo time-course imaging of tumor angiogenesis in colorectal liver metastases in the same living mice using two-photon laser scanning microscopy. J Oncol 2012:265487. doi:10.1155/2012/265487

22. Satsangi J, Silverberg MS, Vermeire S et al (2006) The Montreal classification of inflammatory bowel disease: controversies, consensus, and implications. Gut 55(6):749–753

23. Brill A, Fuchs TA, Savchenko AS et al (2012) Neutrophil extracellular traps promote deep vein thrombosis in mice. J Thromb Haemost 10(1):136–144

24. Fuchs TA, Brill A, Duerschmied D et al (2010) Extracellular DNA traps promote thrombosis. Proc Natl Acad Sci USA 107(36):15880–15885

25. Doring Y, Manthey HD, Drechsler M et al (2012) Auto-antigenic protein-DNA complexes stimulate plasmacytoid dendritic cells to promote atherosclerosis. Circulation 125(13):1673–1683

26. Dubois AV, Gauthier A, Brea D et al (2012) Influence of DNA on the activities and inhibition of neutrophil serine proteases in cystic fibrosis sputum. Am J Respir Cell Mol Biol 47(1):80–86

27. Cools-Lartigue J, Spicer J, McDonald B et al (2013) Neutrophil extracellular traps sequester circulating tumor cells and promote metastasis. J Clin Invest 123(8):3446–3458

28. Saffarzadeh M, Juenemann C, Queisser MA et al (2012) Neutrophil extracellular traps directly induce epithelial and endothelial cell death: a predominant role of histones. PLoS One 7(2):e32366

29. Kohlova M, Ribeiro S, do Sameiro-Faria M et al (2013) Circulating cell-free DNA levels in hemodialysis patients and its association with inflammation, iron metabolism, and rhEPO doses. Hemodial Int 17(4):664–667

30. Keshari RS, Jyoti A, Kumar S et al (2012) Neutrophil extracellular traps contain mitochondrial as well as nuclear DNA and exhibit inflammatory potential. Cytometry A 81(3):238–247

31. Atamaniuk J, Kopecky C, Skoupy S et al (2012) Apoptotic cell-free DNA promotes inflammation in haemodialysis patients. Nephrol Dial Transplant 27(3):902–905

32. Margraf S, Logters T, Reipen J et al (2008) Neutrophil-derived circulating free DNA (cf-DNA/NETs): a potential prognostic marker for posttraumatic development of inflammatory second hit and sepsis. Shock 30(4):352–358

33. Jylhava J, Nevalainen T, Marttila S et al (2013) Characterization of the role of distinct plasma cell-free DNA species in age-associated inflammation and frailty. Aging Cell 12(3):388–397

34. Yang D, Oppenheim JJ (2004) Antimicrobial proteins act as "alarmins" in joint immune defense. Arthritis Rheum 50(11):3401–3403